Structure–property behaviour of segmented poly(tetramethylene oxide)-based bipyridinium ionene elastomers

Daan Feng*, Garth L. Wilkes*, Bin Lee†‡ and James E. McGrath†
**Department of Chemical Engineering, †Department of Chemistry, and*
**†Polymer Materials and Interface Laboratory, Virginia Polytechnic Institute &*
State University, Blacksburg, Virginia 24061-6496, USA
(*Received 3 August 1990; accepted 14 October 1990*)

Structure–property behaviour of poly(tetramethylene oxide) (PTMO)-bipyridinium ionene elastomers have been investigated. These systems display high tensile properties and high elongation. Their general properties can be explained as being due to the high degree of microphase separation of ionic domains promoted by strong coulombic interactions in conjunction with strain induced crystallization of the PTMO soft segments. The microphase separation was established by use of small angle X-ray scattering as well as limited use of transmission electron microscopy. Some indication of the thermal stability characteristics of these materials is also presented.

(Keywords: ionene; elastomer; ionomer; poly(tetramethylene oxide); segmented copolymers; block copolymers)

INTRODUCTION

Ionenes are polymers in which macromolecules contain cationic quaternary amines as integral links in the polymer backbone. In 1968, Rembaum *et al.*[1] prepared a variety of high-molecular-weight aliphatic ionenes by the Menschutkin reaction and defined the term 'ionene' for this type of polymer. Since then, ionene polymers prepared by different routes have received increasing attention as potential components in conductive polymers, photovoltatic cells, cosmetics, water treatment flocculants, etc. However, most of the objectives of these previous studies have concerned the solution and electrical properties of aliphatic ionenes[1–12].

In recent years, elastomeric ionomers prepared by ionene chemistry have also gained attention[10–21]. While the ionene elastomers may vary in the type of ionene moieties (ionic hard segment) and soft segments, they often display very high tensile strength and high elongation. Recently, the structure–property behaviour of poly(tetramethylene oxide) (PTMO)-benzyl dihalide ionene systems has been investigated in our laboratory[21–23]. In these systems, PTMO was utilized as the soft segment and a benzyl dihalide compound as the hard segment[19,20]. The results indicate that the excellent tensile properties of these novel materials result from a very high degree of microphase separation (ionic domain formation). The microphase separation is driven by strong ionic interactions present in these systems. Owing to these interactions, a long-range ordered continuous domain structure is formed even at relatively low volume fraction of the ionic hard segments (ca. 7 vol%). As expected, the nature of the ionic domain structure and the bulk properties of the PTMO–dihalide ionene elastomers are altered with ionic content, the type of counterion or the type of ionic hard segments.

Currently, another type of PTMO-based ionene elastomer has been investigated in our laboratories. These PTMO–bipyridinium ionenes are prepared by the coupling reaction of 'living' polytetrahydrofuran dioxonium ions with either 4,4′-bipyridine or 1,2-bis(4-pyridinium)ethylene. The synthesis of the PTMO–bipyridinium ionene polymers is outlined below:

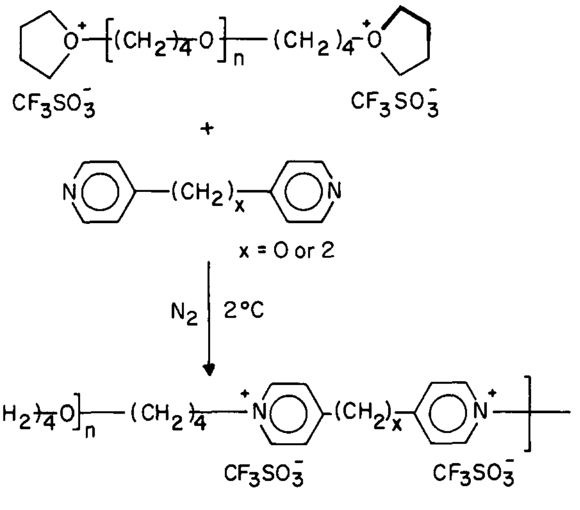

In 1985, Kohjiya *et al.*[24] first utilized 4,4′-bipyridine to terminate living PTMO dioxonium ions. However, they were only interested in the polyelectrolyte and photochromic behaviour of these materials. The structure–property behaviour of these materials was not reported.

Without an awareness of the work of Kohjiya *et al.*, Lee *et al.*[25,26] also developed the same type of

---

‡ Current address: Mobay Chemical Co., Pittsburgh, Pennsylvania, USA

0032-3861/92/030526-10

PTMO–bipyridinium ionenes by the same synthesis procedure. N.m.r. studies confirmed that the segmented ionene polymers were formed[26]. Preliminary structure–property studies[26,27] indicated that a well defined microphase separation developed in these materials. The mechanical properties of the PTMO–bipyridinium ionene were in many respects quite similar to those of the PTMO–benzyl dihalide ionenes. However, thermal mechanical results indicated that the PTMO–bipyridinium ionenes had a much higher softening temperature (ca. 210°C) than the PTMO–benzyl dihalide ionenes (ca. 175°C) and the former were less susceptible to thermal degradation when thermally processed.

In this article, the structure–property behaviour of the PTMO–bipyridinium ionene polymers will be discussed. The discussion will focus on information accounting for the characteristics of these materials as a function of the PTMO soft segment molecular weight and the architectural differences of the ionene hard segment components.

EXPERIMENTAL

Sample preparation and designation

The synthesis of the PTMO–bipyridinium ionene polymers that will be discussed here have been described elsewhere[25,26]. The polymer films were solution cast from either methanol or acetone. The casting was performed at room temperature for 3–4 days. The films were then dried at 60°C *in vacuo* and were stored in a vacuum desiccator until tested. Besides solution-cast films, a thermal compression-moulded film was also prepared. This film was pressed at 230°C (which was only 10°C higher than the softening temperature of the polymer) for 5 min to minimize the degradation of the PTMO soft segment. Then the film was quenched and stored under vacuum until tested.

To provide information on the molecular weight of the PTMO soft segments, the type of counterion and ionene hard segment, the following sample designation will be used:

IS - BP - 25
↑ ↑ ↑
PTMO segment $M_n/100$
Type of hard segment
(BP = bipyridinium, BPE = bipyridinium ethane)
Type of counterion (S = triflic acid anion)

Additional composition information regarding these materials is listed in *Table 1*.

Methodology

The tensile stress–strain behaviour of the ionene materials was measured on an Instron 1122 tester at ambient temperature (23–25°C and ca. 50% relative humidity) with a crosshead speed of 50 mm min^{-1}. Dogbone specimens were of dimensions 2.8 mm in width and 10 mm in gauge length. Mechanical hysteresis behaviour was measured by repeated cyclic stress–strain measurements. The cycles were carried out at elongation values of 10, 20, 30, 50, 100, 200, 300 and 500%. Each loading cycle was initiated when the crosshead returned to the starting position of the undeformed sample from the previous cycle. The loading and unloading crosshead speed was 50 mm min^{-1}. The specimen dimensions and the testing conditions for the hysteresis experiments were the same as for the stress–strain measurements.

Thermal analysis, differential scanning calorimetry (d.s.c.), thermal mechanical analysis (t.m.a.) and thermogravimetry (t.g.a.) were carried out on a Seiko SSC5000 thermal analysis system. The data were collected at a heating rate of 10°C min^{-1}. For the d.s.c. and t.m.a. the temperature range utilized was from −150 to 250°C. A *flat-tip penetration probe* was used for the t.m.a. measurement with a loading of 20 g. The t.g.a. measurements were carried out from 25 to 550°C. All thermal measurements were performed in a nitrogen environment.

The dynamic mechanical response of these ionene systems was monitored by an automated Rheovibron DDV-II-C over a temperature range from −150 to 200°C. The measurements were made at a frequency of 11 Hz with a heating rate of 2°C min^{-1}. All measurements were carried out under a purging dry nitrogen stream to eliminate moisture condensation.

The microphase structure of the ionene polymers was investigated by utilizing X-ray scattering techniques in both the small-angle and wide-angle regions. Small-angle X-ray scattering (SAXS) was performed on an automated Kratky slit-collimated camera. The scattering intensity was monitored by a one-dimensional Braun position-sensitive detector. In addition, a simple Warhus camera with pinhole collimation utilizing a flat-plate film cassette was used for both small- and wide-angle X-ray scattering studies. All X-ray scattering experiments were at ambient temperature.

Besides X-ray scattering, transmission electron microscopy (TEM) was also utilized to study the morphology.

Table 1 Composition of PTMO–bipyridinium ionene elastomers

Sample	PTMO segment M_n	Ion content (no. ions/PTMO unit)	Hard segment wt% (w ion)	Hard segment wt% (w/o ion)
IS–BP–6	550	0.26	44	22.1
IS–BP–8	750	0.19	37	17.2
IS–BP–13	1350	0.11	25	10.4
IS–BP–17	1700	0.09	21	8.4
IS–BP–25	2550	0.07	15	5.8
IS–BPE–13	1350	0.11	26	12.0
IS–BPE–18	1800	0.08	21	9.3
IS–BPE–25	2500	0.06	18	7.7

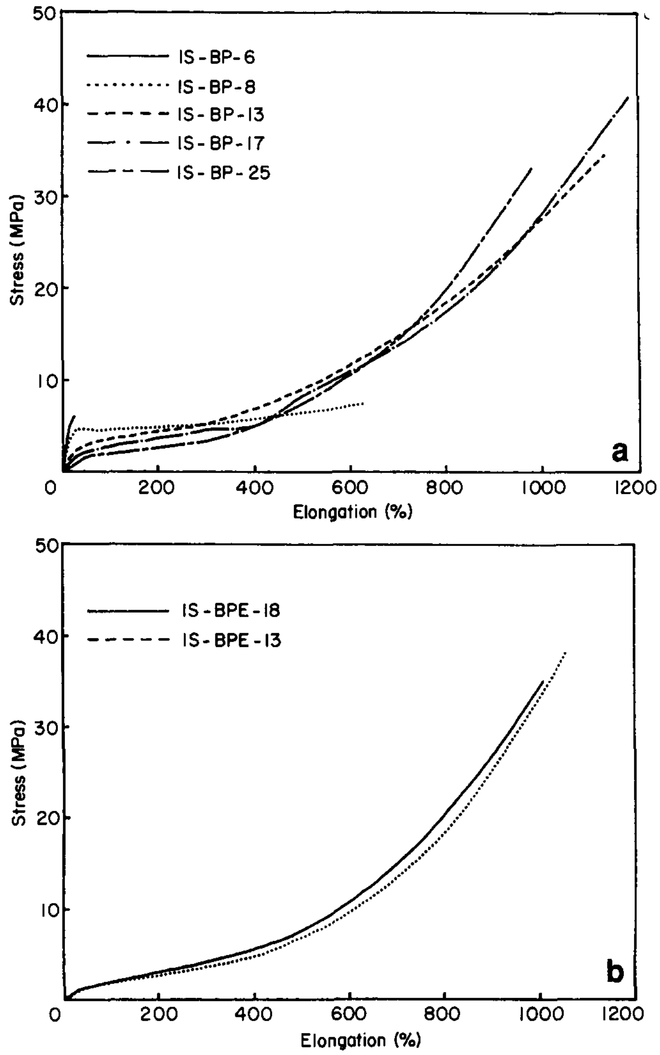

Figure 1 Stress–strain behaviour of the PTMO–bipyridinium ionene elastomers: (a) the IS–BP series; (b) the IS–BPE series

The TEM studies were done on a JEOL 200CX transmission electron microscope with an acceleration voltage of 200 kV. Cryomicrotomed ultrathin sections were made from the *same polymer films* as were used in the mechanical, thermal and X-ray scattering measurements. Owing to the high electron density difference between the two different segments, sufficient contrast existed without the need for selective staining.

RESULTS AND DISCUSSION

Mechanical properties of the IS ionene elastomers

The general stress–strain behaviour of the solution-cast PTMO–bipyridinium (IS) ionene films is shown in *Figure 1*. Some of these materials exhibit excellent elastomeric properties as well as high tensile strength and high elongation. As the PTMO soft segment molecular weight decreases, the Young's modulus as well as the stress level at a given elongation level increase. Since the ionic content of the IS ionene elastomers increases as the PTMO soft segment molecular weight decreases, the increase in the moduli and the stress level results from an increase in the ionic content[21]. When the elongation level exceeds 600%, a distinct stress upturn is observed. It is primarily due to the strain-induced crystallinity in the PTMO soft segments and has been proven by wide-angle X-ray scattering (data not shown here). In contrast to the stress–strain behaviour at lower elongation ($<500\%$), the stress level increases with an increase in the PTMO soft segment molecular weight (for a given elongation) at high elongation levels. It is speculated to be caused by a higher level of strain-induced crystallinity for the longer PTMO soft segments. There was no casting solvent dependence observed on the stress–strain behaviour for these materials.

The stress–strain behaviour of the IS–BP systems as well as the IS–BPE systems are very similar (see *Figure 1*). This indicates that the type of ionic hard segment architecture has little major effect on the stress–strain properties, other factors being similar.

As shown in *Figure 1a*, samples IS–BP–6 and IS–BP–8 behave differently compared to other samples, such as high modulus and low elongation. This is believed to result from a higher ionic content. As the PTMO soft segment molecular weight decreases, the ionic content increases. Consequently, the ionic interaction increases and the modulus increases[21]. The low elongation of these two samples is believed to be due to the relatively low molecular weight of these polymers[26]. In fact, during the synthesis, the termination process is much more rapid for the ionenes containing shorter PTMO segments owing to the higher concentration of ionic species possibly promoting premature precipitation to occur. Hence, the molecular weight of the final polymer may be somewhat lowered[26].

The mechanical hysteresis data obtained on samples IS–BP–17 and IS–BP–25 are given in *Figure 2*. This plot illustrates that, at ambient temperature, there is a difference in their dissipative character. Sample IS–BP–17 has a higher percentage hysteresis than that for sample IS–BP–25. The percentage hysteresis for these PTMO–bipyridinium ionene systems is relatively high at least compared to elastomeric sulphonated telechelic polyisobutylene ionomers investigated in this same laboratory under identical conditions[28]. However, in the latter system, the stress levels were considerably less than for the ionene systems. Also, the hysteresis behaviour of the PTMO–bipyridinium ionenes is quite similar to that found for PTMO–benzyl dihalide ionenes of comparable PTMO segment molecular weights and several other thermoplastic segmented polyurethanes that have also

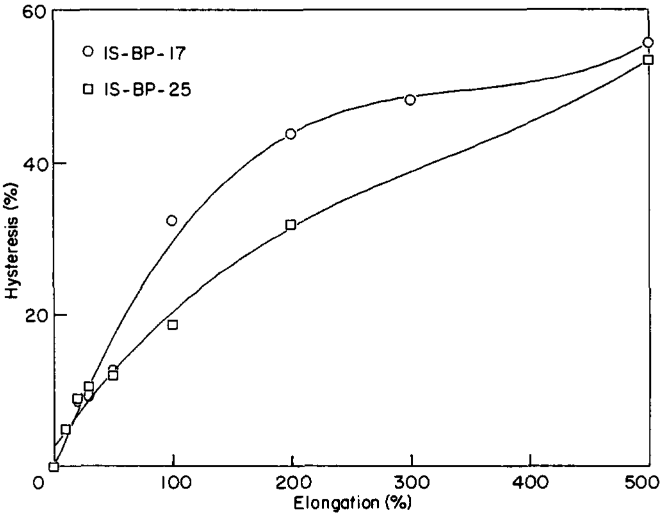

Figure 2 Mechanical hysteresis behaviour of the PTMO–bipyridinium ionene elastomers

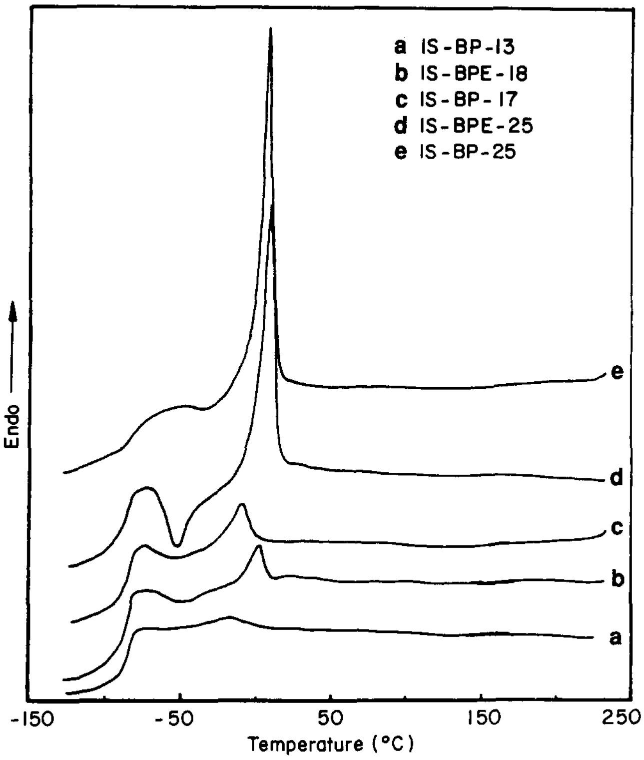

Figure 3 D.s.c. thermograms of the PTMO-bipyridinium ionene elastomers

been investigated in this laboratory[23,29]. Besides the relatively high hysteresis, samples IS–BP–17 and IS–BP–25 also display 30% and 20% permanent set respectively after they have been stretched to 300% elongation. The high hysteresis and permanent set of these samples are believed to relate to PTMO chain extension and ionic domain disruption as will be discussed in later sections of this paper.

Thermal properties of the IS ionene elastomers

Figure 3 shows the d.s.c. thermograms of both IS–BP and IS–BPE ionene polymers. Three transitions are observed: the glass transition (ca. −80°C), the crystallization (ca. −50°C) and the melting (ca. 5°C) of the PTMO segments. The T_g values of the PTMO soft segments are the same as the PTMO homopolymer, although a slight molecular-weight dependence is noted. This suggests that the degree of phase separation of the soft segment from the ionene moieties is very high, otherwise the T_g of the PTMO soft segments would be shifted upwards. The glass transition temperature of the PTMO soft segments is also independent of the soft segment molecular weight and either type of hard segment.

The crystallization and the melting behaviour of the PTMO soft segments is strongly influenced by the soft segment molecular weight as well as the type of the ionic hard segment. In general, the crystallization temperature T_c decreases and the melting temperature (T_m) increases as the PTMO soft segment molecular weight increases. The former trend is believed due to end-group restrictions imposed by the ionic domains[26]. As the soft segment molecular weight increases, the distance between the ionic hard segments increases, while the hard segment concentration also decreases. The end-group restriction or end-group effect in the PTMO soft segments will be reduced as the soft segment molecular weight increases. Hence, the PTMO soft segments become more mobile and more readily crystallizable, which may explain the shift of T_c towards a lower temperature. Meanwhile, the melting temperature (T_m) also increases. As a result, the supercooling (temperature range between T_m and T_c) broadens, which facilitates the crystallization of the PTMO soft segments. For example, sample IS–BP–25 has the smallest change in the heat capacity (ΔC_p) at its glass transition than for the other samples. The value of ΔC_p is directly proportional to the amorphous content of the PTMO segments. Since sample IS–BP–25 can crystallize more rapidly during cooling prior to the d.s.c. measurements, this sample would be expected to have higher initial crystallinity than the others. Therefore, it should have the smallest value of ΔC_p. Indeed, this is the case—see *Figure 3*. There is almost no crystallization or melting behaviour observed for sample IS–BP–13 because of its very short PTMO segments.

Dynamic mechanical behaviour of the IS ionene elastomers

The dynamic mechanical spectra of both IS–BP and IS–BPE ionene elastomers are shown in *Figure 4*. Four transitions, α, γ, β_1 and β_2 are observed in the tan δ spectra. The α transition, which occurs at ca. −80°C, is due to the glass transition of the PTMO soft segments. These results are similar to the d.s.c. results. At this transition, the storage moduli (E') of these systems decrease. Depending on the PTMO soft segment molecular weight, the changes in E' at the glass transition ($\Delta E'$) are different. The value of $\Delta E'$ for sample IS–BP–25 is much less than for the other three samples, which is believed to be due to a higher crystallinity of the PTMO soft segments induced during cooling of this specific sample to −150°C. Recall that the cooling rate is approximately 2–3°C min^{-1}, which allows the PTMO to crystallize during cooling. The sample with larger PTMO soft segments such as IS–BP–25 can crystallize more quickly and leads to a higher degree of crystallinity. As a result, the value of $\Delta E'$ at the glass transition for this sample is smaller. Also, the intensity of the α peak is much lower because the intensity of the α peak is proportional to the amount of amorphous PTMO.

The γ transition at −120°C is due to the movements of coupled methylene units in the PTMO backbone and its value is in excellent agreement with the reported values for this same transition observed in polymers possessing methylene sequences in the backbone[32].

The β_1 transition results from the melting behaviour of the PTMO soft segments. The β_1 peak intensity increases as the PTMO soft segment molecular weight increases. Since the intensity of the β_1 peak depends on the level of crystallinity of the PTMO soft segment, a higher intensity indicates a higher level of PTMO crystallinity. Sample IS–BP–8 has the lowest β_1 peak, the lowest E' at the β_1 transition and a high-intensity α peak, which is proportional to the amorphous PTMO content. All responses indicate that the crystallinity in this sample is low because of low PTMO soft segment molecular weight. In contrast, sample IS–BP–25 should have a higher level of PTMO crystallinity because of higher PTMO segment molecular weight. Indeed, it has a higher β_1 peak and a higher value of E' at the β_1 transition region.

The denoted transition β_2 occurs around 50°C. At this transition, the value of E' surprisingly jumps upwards by about a factor of 5! As the ionic content increases (i.e.

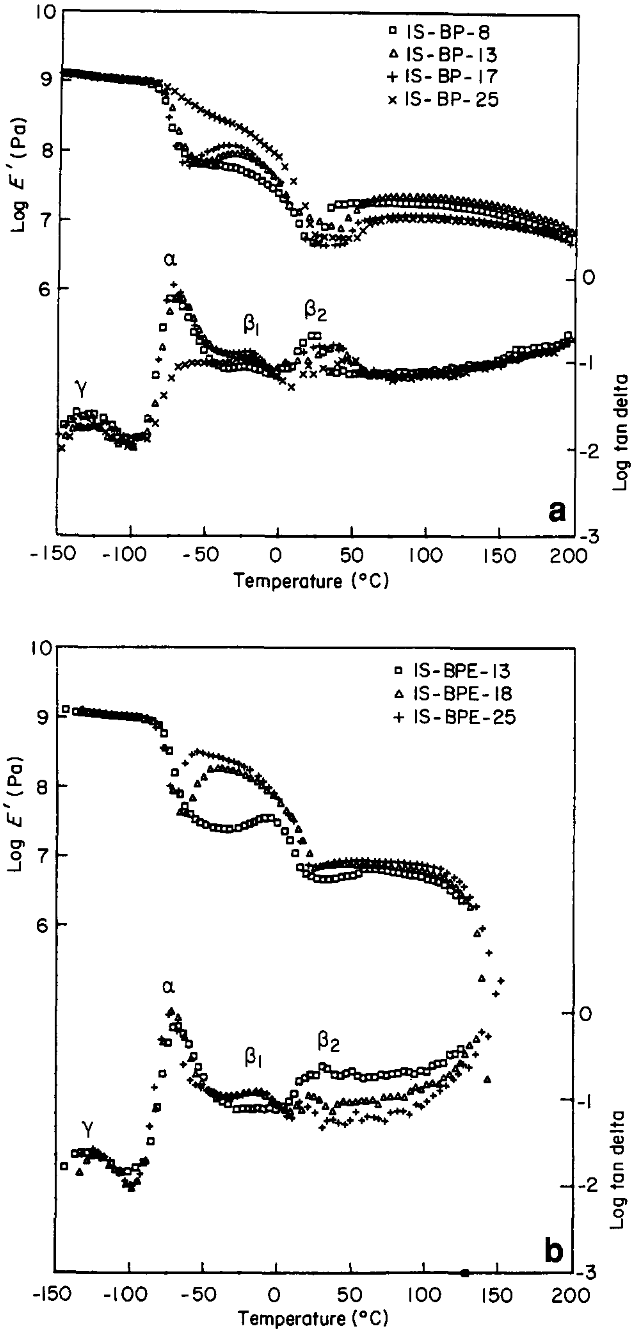

Figure 4 Dynamic mechanical spectra of the ionene elastomers: (a) IS-BP series; (b) IS-BPE series

as the PTMO soft segment molecular weight decreases), the amplitude of the 'jump' in E' increases, while the 'jump' temperature (T_j) shifts to a slightly lower temperature. Interestingly, the 'jump' is *highly reversible*! When the sample is cooled below T_j, the value of E' decreases back to its original level, yet when the sample is heated above T_j, E' moves upwards again. This unusual phenomenon or modulus 'jump', has also been observed in some PTMO–benzyl dihalide ionene systems in which dibromoxylene is utilized as the hard segment, as described elsewhere[23]. It is noteworthy that no such modulus 'jump' has been reported for other ionene systems with different types of soft segments or hard segments[17,18]. By careful inspection of the d.s.c. and d.m.a. data for the IS–BP samples, we have noticed that the difference between the values of T_m and T_j for a given sample is ca. 34°C. We are, however, unable to explain the physical significance of this thermal window. Careful studies indicate that the modulus 'jump' is *not due* to the adsorption–desorption of adsorbed moisture or residual solvent (the measurements were made in a dry nitrogen environment). For both PTMO–benzyl dihalide and PTMO–bipyridinium ionene elastomers, the 'jump' is directly related to the ionic content, type of counterion, hard segment architecture and distance between the charge centres (distance between two positive charged nitrogen atoms in the ionic hard segment). Based on the experimental data, the 'jump' is *speculated* to be caused by conformational changes in the ionic hard segments, rearranging or repacking of ionic hard segments in the ionic domains[23,26].

There is another transition that is not shown in the tan δ spectra of the IS–BP samples owing to the limitations of the instrument. This transition is due to the softening of the samples that occurs at ca. 210°C.

The d.m.a. spectra of the IS–BPE series are similar to the IS–BP series in the *low-temperature* range (<10°C, see *Figure 4b*). However, there is no modulus 'jump' observed for IS–BPE–18 and IS–BPE–25, and only a small sign of the 'jump' is observed for sample IS–BPE–13. Another major difference between the IS–BP and the IS–BPE ionene elastomers is the softening temperature. This temperature of the IS–BPE series is ca. 125°C while it is well in excess of 200°C for the IS–BP samples. In the IS–BPE ionene elastomers, the ionic association may well be weakened by introducing two methylene units in the hard segments; thus the interchain interaction may be lessened and the softening temperature reduced.

Figure 5 shows the t.m.a. properties for samples IS–BP–17 and IS–BPE–18. The transition at −75°C is assigned to the glass transition of the PTMO segments. The transition at ca. 10°C is due to the melting of the PTMO crystallites, which causes an expansion in volume. The last transition occurs at 220°C for sample IS–BP–17 and at 130°C for sample IS–BPE–18. This transition is due to the softening of the ionene elastomers. It also confirms that the softening temperature of the IS–BP series is too high to be observed by d.m.a. According to the t.m.a. results, the softening temperature of these ionene systems is well below their degradation temperature (ca. 280°C, as will be shown later in *Figure 6*). These data indicate that a physically crosslinked

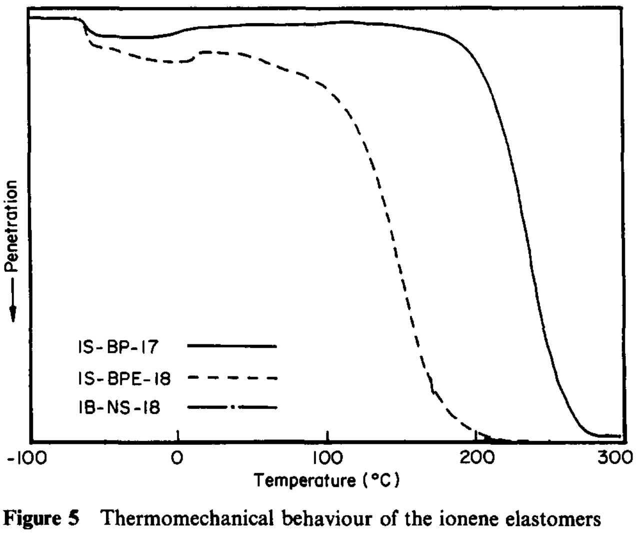

Figure 5 Thermomechanical behaviour of the ionene elastomers

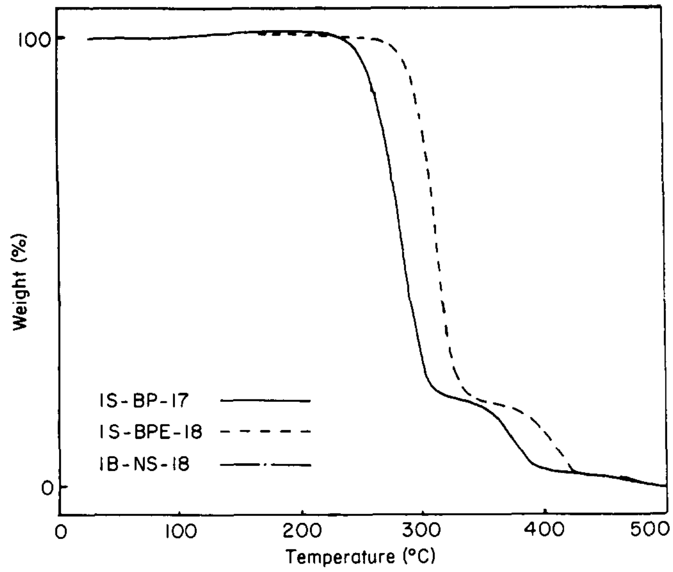

Figure 6 T.g.a. thermograms of the PTMO–bipyridinium ionene elastomers

network is formed in these ionenes instead of a chemically crosslinked network. If a chemically crosslinked network had been formed, the polymers may not soften further from the rubbery state until they begin to degrade; therefore, the softening temperature may be close to the degradation temperature. Since these ionenes are soluble in common solvents such as methanol and acetone, clearly only a physical network accounts for the observed behaviour of these novel thermoplastic elastomers.

Thermal stability and thermal processibility

The thermal stability of the IS ionenes is illustrated by the t.g.a. thermograms shown in *Figure 6*. Two major weight losses are observed in each t.g.a. curve. For sample IS–BP–17, a primary catastrophic weight loss occurs at 280°C. This weight loss may be due to the decomposition of the PTMO segments, and the secondary weight loss occurs at ca. 400°C, which may be due to further degradation of the hard segment. For sample IS–BPE–18, the primary weight loss occurs at 310°C. In fact, all IS–BPE ionenes have higher decomposition temperatures than the analogous IS–BP samples[25]. The better thermal stability of the IS–BPE sample may be at least partially due to the charge separation of the two single positive charges in the hard segment. The further apart these charges are, the more stable the polymer appears to be[26]. In addition, one would also expect the presence of the benzylic methylene to limit thermal and thermal/oxidative behaviour.

Our t.g.a. results (not shown here) for a hydroxyl-terminated PTMO oligomer ($M_w = 2900$) shows that a complete weight loss occurs at 180°C. This has been accounted for by the degradation through unzipping of the PTMO oligomer[33]. Since the initial decomposition temperatures for the ionene polymers well exceed 250°C, the improvement of thermal stability is probably due to the effect of different functional end-groups. Recent thermal degradation studies found that the thermal stability of poly(propylene oxide) (PPO) was also strongly influenced by the type of end-groups[39]. In the ionene polymers, the PTMO soft segments are connected by ionic hard segments, which can be regarded as the functional end-groups. Therefore, when the type of ionic hard segment changes, the thermal stability of the ionene is expected to change also.

One very important feature of the PTMO–bipyridinium ionenes is their thermal processibility, which has been demonstrated by the stress–strain behaviour of a thermally moulded film of sample IS–BP–25. The film was thermally pressed at 230°C, which is 10°C higher than the softening temperature, for 5 min to minimize the degradation. Then, the film was quenched to 65°C. The tensile specimens were cut at different times after the sample has been quenched. The results in *Figure 7* illustrate a time-dependent recovery of the tensile properties for sample IS–BP–25. The film does recover some of its initial mechanical properties 5 min after moulding. Thirty-six minutes after moulding, the tensile strength is over half of the value of the solution-cast film of the same sample. Fifteen hours after moulding, the tensile strength of the moulded film reaches about three-quarters of the tensile strength of the solution-cast film. The thermal processibility of the PTMO–bipyridinium ionenes is believed to result from their chemical nature. These materials are prepared by a coupling reaction, which is not a reversible process. Therefore, the PTMO–bipyridinium ionenes retain at least the majority of their chemical chain structure at elevated temperature. However, an interesting feature is the time-dependent recovery process of the stress–strain behaviour of the IS ionene polymer. This may be caused by a slow possible reforming process of the ionic domains following quenching from the melt, a topic that is now being investigated. Also, the thermal moulded film did not totally recover its properties relative to the solution-cast film. This may be due to partial degradation of the polymer during the thermal moulding. After thermal moulding, a light brown colour develops in the film. The colour is believed to arise from partial degradation of the PTMO soft segment during thermal moulding, since there was no antioxidant added in these ionenes. Another possibility for the colour change is due to the occurrence of oxidation of the bipyridinium unit, which is a known viologen. As a point of comparison, our earlier studies with the PTMO–benzyl dihalide systems indicate that the PTMO–benzyl dihalide ionenes *cannot* be thermally processed at all in the neat state because they are prepared

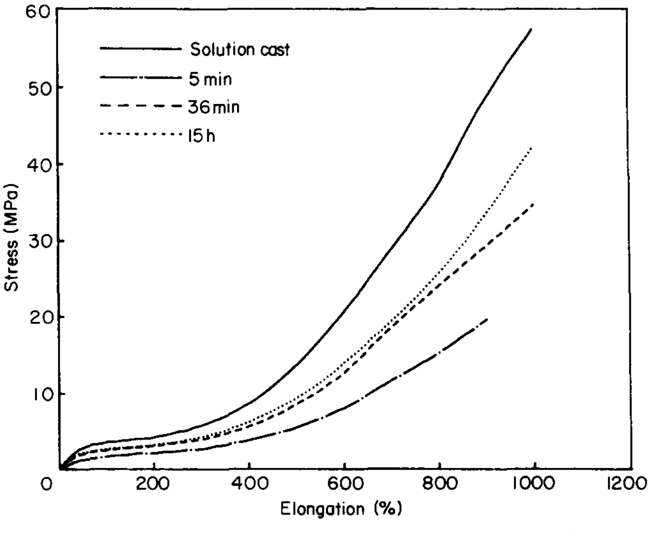

Figure 7 Stress–strain behaviour of thermally moulded films of IS–BP–25

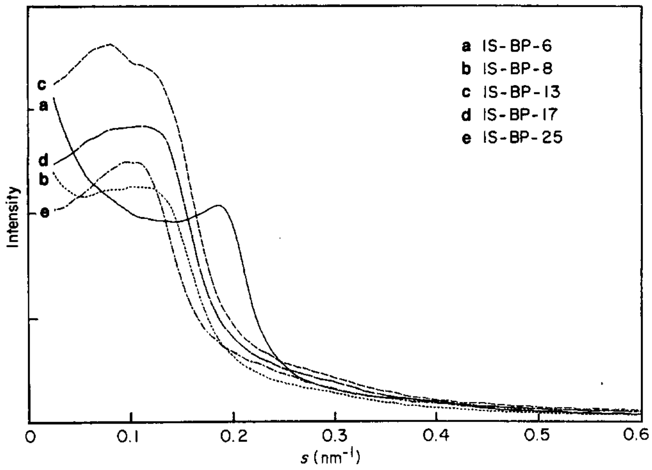

Figure 8 SAXS profiles of the IS–BP ionene elastomers: s is the scattering vector and $s = (2/\lambda)\sin\theta$

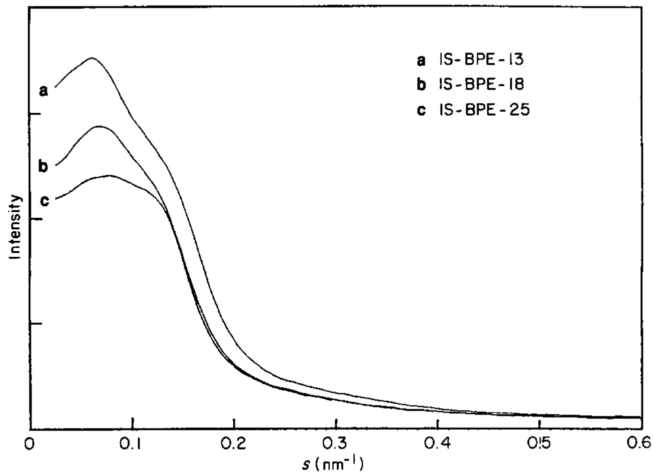

Figure 9 SAXS profiles of the IS–BPE ionene polymers

by the Menschutkin reaction, which leads to depolymerization and other side reactions at an elevated temperature (ca. 170°C)[23].

Morphological texture of the IS ionene polymers

To confirm the occurrence of the ionic domain formation in these IS ionene materials, small-angle X-ray scattering (SAXS) and transmission electron microscopy (TEM) have been utilized. *Figures 8* and *9* show the smeared SAXS profiles of these ionene polymers. There is a very distinct and broad scattering peak in each SAXS profile, which indicates the presence of microphase separation or ionic domain formation.

From the SAXS results, the estimated interdomain spacing (d spacing), which is calculated from the location of the peak, changes with the PTMO soft segment molecular weight for the IS ionenes. The d spacing estimated from the *smeared* SAXS profiles is in a range from 7 to 12 nm as listed in *Table 2*. It is necessary to point out that it is difficult to determine accurately the d spacing from the SAXS profiles owing to the broadness of the SAXS peaks. Therefore, the values listed in *Table 2* are estimated values. Also, owing to the smearing effect, the estimated d spacing is always somewhat larger than the true values. However, comparisons can still be made between the different ionene samples.

As shown in *Figure 8* and *Table 2*, the d spacing of the IS–BP ionenes does increase with an increase in the PTMO soft segment molecular weight when the molecular weight is less than 1300 g mol^{-1}. Above this, the d spacing surprisingly seems to decrease slightly as the PTMO segment molecular weight increases to 2500. In our earlier studies of the PTMO–benzyl dihalide ionene systems, the SAXS peak was clearly shown to arise from the interdomain scattering. Those systems have identical PTMO soft segments, as described elsewhere[22]. Therefore, the d spacing for the present PTMO–bipyridinium ionenes was expected also to increase with the PTMO soft segment molecular weight. One possible explanation for this deviation from the expected behaviour may be due to enhanced PTMO chain extension in the present materials, as discussed below.

For the ionene elastomers, strong coulombic interactions exist between the polymer chains through the ionic hard segments. The ionic hard segments attract each other to form ionic domains and the PTMO segments between the hard segments may be partially stretched. The level of coulombic interactions increases with an increase in ionic content resulting from the decrease in PTMO soft segment molecular weight. As a result, the PTMO soft segments, which connect the ionic hard segments, may be more extended for the sample containing lower PTMO segment molecular weight. To shed further light on this assumption, the interdomain spacing for two *extreme* cases has been considered, the first being the fully extended state of the PTMO segments and the other case being where the PTMO segments are considered to be gaussian coils. Since the number of bonds per PTMO segment is well over 50 in these IS ionenes, the gaussian assumption seems quite reasonable[34].

For the *fully extended* PTMO segment, the interdomain spacing d_s is estimated as follows:

$$d_s = D + N \sum n_i l_i \sin(\theta_i/2) \qquad (1)$$

where D is the length of hard segment, which is 0.77 nm for the BP unit and 1.13 nm for the BPE unit calculated from their molecular structures; N is the number of repeat units per PTMO soft segment; n_i is the number of ith type bonds per repeat unit (for a PTMO repeat unit, there are four C–C bonds and one C–O bond); l_i and θ_i are the bond length and the bond angle for the ith type bond (for the C–C bond, l_i is 0.154 nm and θ_i is 109°; the C–O bond has values of 0.150 nm and 90° for l_i and θ_i respectively).

Table 2 Interdomain spacings of IS–BP and IS–BPE ionene polymers[a]

Sample	d (nm)	d_s (nm)	d_s/d	d_g (nm)
IS–BP–6	5.3	5.8	1.1	1.8
IS–BP–8	8.2	7.5	0.9	2.1
IS–BP–13	12.3	11.8	1.0	4.3
IS–BP–17	8.7	15.1	1.7	4.7
IS–BP–25	9.2	21.9	2.4	5.6
IS–BPE–13	16.2	12.1	0.8	4.6
IS–BPE–18	14.9	16.3	1.1	5.5
IS–BPE–25	12.8	21.2	1.7	6.0

[a] The hard segment length is estimated as 0.8 nm for BP and 1.1 nm for BPE

For a *gaussian* PTMO segment, the interdomain spacing d_g can be estimated from the unperturbed root-mean-square end-to-end distance (RMS), which has been estimated by[35]:

$$RMS = \left(CN \sum n_i l_i^2 \right)^{1/2} \quad (2)$$

where C is the characteristic ratio and is 5.7 for PTMO[31]. Therefore, the value of d_g becomes:

$$d_g = D + RMS \quad (3)$$

The calculated values of d_s and d_g are listed in *Table 2* along with the d spacing calculated from smeared SAXS profiles.

The results indicate that the d_g values estimated from the gaussian calculation (equations (2) and (3)) are far below the d spacing values measured from the SAXS profiles. Therefore, the gaussian assumption is not a suitable one because of the presence of strong ionic interaction and very low PTMO soft segment molecular weight. Yet, the values of the d spacing obtained from SAXS are quite close to the d_s values calculated from equation (1). As the PTMO soft segment molecular weight increases, however, the difference between d_s and d increases. The values of d become distinctly smaller than d_s. This indicates that the PTMO soft segments become more gaussian-like as the segment molecular weight increases (> 1800 g mol^{-1}), as might be expected. Hence, these results do imply that the PTMO segments in these PTMO–bipyridinium ionenes may be extended—particularly for the lower-molecular-weight soft segments. The authors find this rather surprising since the macroscopic elongation of these materials should be due to the PTMO soft segment chain extension under load. If the PTMO segments are already highly extended, how can these materials still be stretched to 1000% elongation? One possible cause is disentangling of the polymer chains and the disruption–rehealing of the ionic domains. This assumption is supported by recent deformation studies on the PTMO–benzyl dihalide ionenes. It has been identified that the SAXS peaks for the PTMO–benzyl dihalide ionenes arise from the interdomain scattering, and similar chain extension for the PTMO soft segments is observed[23]. Yet, the results from deformation studies indicate that the d spacings for these systems almost undergo no change when the sample has been uniaxially stretched up to 300% elongation[36]. Similar results have been reported on styrene–butadiene block polymers as well as polyurethane systems, and these results have been attributed to the disentanglement of the polymer chains and the domain distortion for the block polymers[37,38]. Besides, the assumption of disentangled polymer chains and ionic domain disruption can be used to explain the mechanical hysteresis behaviour and the permanent set. If the ionic domains are disrupted, the percentage hysteresis will be higher, and the permanent set will be as observed.

The reader should keep in mind that the measured d spacing was estimated from the smeared SAXS data. In general, the smeared data will yield a larger d spacing than its actual value. Also, the molecular-weight distribution of the PTMO segments has not been taken into account in the above discussion. Considering these two factors, the degree of chain extension is therefore slightly smaller than discussed above.

Another possible explanation for the SAXS behaviour of the IS ionenes is that the scattering peak may arise from *intradomain* scattering rather from *interdomain* scattering. However, this hypothesis lacks experimental support. If the SAXS peak arises from intradomain scattering, one might expect that the domain size would decrease with ion content owing to a decrease in the number of ionene units per ionic domain as influenced by hard segment accessibility. The SAXS results, however, illustrate that the d spacing distinctly decreases with the PTMO soft segment molecular weight when the PTMO segment molecular weight is below 1300 g mol^{-1}. Above 1300 g mol^{-1}, the change in the d spacing is not very pronounced with changes in PTMO soft segment molecular weight. Therefore, it is difficult to explain the SAXS behaviour of these ionene systems by intradomain scattering. The TEM results to be discussed in a later section indicate that there are no domains with size on the order of 10 nm. Since the d spacing obtained from SAXS data is of the order of 10 nm, the TEM results do *not* support the intradomain scattering assumption. In fact, the TEM results support that the SAXS peaks arise from the *interdomain scattering* as will be shown later.

As noted from *Figure 8*, the broadness of the SAXS peaks also changes with the PTMO soft segment molecular weight in the same order as the d spacing. As the PTMO soft segment molecular weight increases from 600 to 1300 g mol^{-1} (about 8 to 18 PTMO repeat units), the peak becomes broader. When the PTMO soft segment molecular weight increases further, however, the peak narrows again. The changes in peak broadness may be attributed to the factors of either *the molecular-weight distribution and the chain extension* of the PTMO soft segment or *the overall molecular weight* of the polymer. It is speculated that the molecular-weight distribution along with some contributions of chain extension mainly promote the peak broadness of samples IS–BP–13, IS–BP–17 and IS–BP–25. In these ionene systems, the interdomain spacing (d spacing) depends solely on the PTMO soft segment molecular weight because the hard segment is a single unit, and hence there is no hard segment molecular-weight distribution as in the well known thermoplastic elastomeric polyurethanes. When the soft segment has a broad molecular-weight distribution, the d spacing may be broadened, i.e. the scattering peak broadens. However, the relationship between the molecular-weight distribution and the scattering peak broadness also depends on the state of the PTMO soft segments. For example, *if* the soft segments are really distinctly extended, the peak broadness would directly reflect the molecular-weight distribution of the soft segment. Certainly, if the soft segments are in the state of gaussian coils, the molecular-weight distribution of the soft segment would have much less influence on the peak broadness. As discussed in earlier sections, the PTMO soft segments are speculated to be somewhat extended owing to the ionic interactions. When the PTMO segment molecular weight increases, the strength of the ionic interaction decreases because of the decrease in the ion content. Also, the number of PTMO repeat units increases as well (i.e. there are 35 repeat units or 175 primary bonds in the PTMO segments for IS–BP–25). Therefore, the PTMO segments become more flexible and behave more like a gaussian chain. Consequently, the molecular-weight distribution of the PTMO soft segment has less influence on the scattering peak broadness. As a result, the

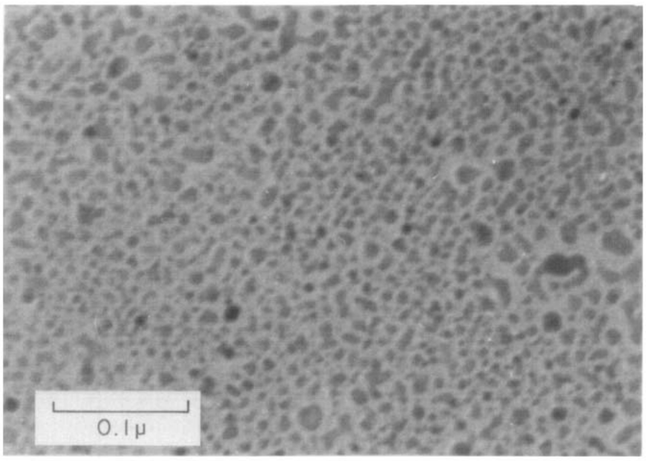

Figure 10 TEM micrograph of sample IS–BP–25

scattering peak narrows as the soft segment molecular weight increases.

In earlier discussions, the poor mechanical properties of samples IS–BP–6 and IS–BP–8 may result from the low overall molecular weight (see *Figure 1*). For these two samples, the dependence of the SAXS peak broadness on the PTMO segment molecular weight may also be due to a lower overall molecular weight of these two ionenes compared to the others. When the overall molecular weight decreases, the number of segments per polymer chain will decrease at constant segment molecular weight. Therefore, a more regular domain structure can be formed. Hence, the SAXS peak becomes narrower. Such behaviour has been reported by Hashimoto *et al.* for styrene–butadiene diblock polymers[30] where these systems are composed of longer coil-like blocks. They have found that, when the molecular weight of the diblock polymer decreases, the scattering peak becomes narrower and more distinct owing to the formation of a much more regular domain structure.

Besides the SAXS profiles, the SAXS patterns of the IS–BP ionene polymers have also been obtained using a pinhole Warhus camera. These patterns result from imposing the X-ray beam on the sample in three orthogonal directions to identify the three-dimensional morphological textures in these materials. Results indicate that the patterns obtained from three directions are identical. There is *no high-order scattering nor is there any azimuthal dependence*. The absence of any high-order scattering peak suggests that there is no long-range ordered domain structure. Instead, the morphological texture of the IS ionene polymers is more likely that of dispersed domains based on the X-ray scattering results and the TEM results discussed in the following paragraph.

Some TEM studies have also been conducted on ultrathin sections of sample IS–BP–25, which displayed the sharpest SAXS scattering peak. *Figure 10* shows the TEM image of sample IS–BP–25 with the electron beam parallel to the film surface. When the electron beam is perpendicular to the film surface, the image is comparable to the image shown in *Figure 10*. A defocusing analysis indicates that the images are not due to artifacts. The observed TEM images are presently believed to be some dispersed domains. The interdomain spacing measured from the micrograph is in the range of ca. 10 nm, which is in good agreement with the SAXS results, while the domain size is also not uniform and the domains are not in an ordered arrangement. This would support the observed broadness of the SAXS scattering peak. Finally, the TEM results indicate that the SAXS peaks have not arisen from intradomain scattering. If the SAXS peak did arise from intradomain scattering, a different scale morphological texture would be expected.

Other properties

Several other interesting features have been observed in the IS ionene elastomers. One of these is their photochromic behaviour. When a methanol cast film of IS–BP polymer is exposed to light for a period of time (several weeks), the initially clear film changes to a brown colour even though the film is stored in a vacuum desiccator during the exposure period. After recasting the film from methanol, the colour disappears. Also, the colour is regenerated if the film is exposed to light again. The photochromic phenomenon of PTMO–bipyridinium ionene has been reported by Kohjiya *et al.*[24]. Since the photochromic phenomenon was not a major focus of this study, no further work was undertaken to examine this behaviour. However, future investigations of this behaviour may be of interest.

SUMMARY

The general structure–property behaviour of PTMO–bipyridinium ionene elastomers is similar to other ionene elastomers that have been reported in the literature. The high tensile properties of these ionenes are due to a high degree of microphase separation and the formation of ionic domains promoted by the strong ionic interactions in conjunction with the strain-induced crystallization of the PTMO soft segments. A major advantage of these materials is that they can be thermally processed without complete loss of their mechanical properties.

The SAXS profiles of the IS ionene polymers contain a single broad scattering peak, which indicates ionic domain formation. Since there are no higher-order scattering peaks observed, the results suggest that these systems are probably randomly dispersed ionic domains. Limited TEM results indicate that the domain structure in sample IS–BP–25 is randomly dispersed domains in a non-ionic matrix.

A reversible modulus 'jump' with temperature is observed for the IS–BP ionene polymers. The amplitude and the location of the 'jump' vary with the ionic content. As the PTMO segment length increases or the ionic content decreases, the amplitude of the modulus rise decreases, and its onset shifts to a higher temperature. Based on d.m.a. results, the modulus rise is also dependent on the hard segment architecture. When two methylene units are introduced into the hard segment, the rise almost disappears, which suggests that it may relate to a possible conformation change in the ionene segments.

ACKNOWLEDGEMENT

The authors would like to acknowledge the partial financial support of this work by the Army Research Office under Grant No. DAAG29-84-0091.

REFERENCES

1 Rembaum, A., Baumgartner, W. and Eisenberg, A. *J. Polym. Sci., Polym. Lett.* 1968, **6**, 159

2 Hadek, V., Noguchi, H. and Rembaum, A. *Macromolecules* 1971, **4**, 494

3 Casson, D. and Rembaum, A. *Macromolecules* 1972, **5**, 74

4 Buruiana, T., Bestiuc, I. and Caraculacu, A. *Angew. Makromol. Chem.* 1987, **147**, 99

5 Buruiana, T., Bestiuc, I., Popescu, V. and Caraculacu, A. *Angew. Makromol. Chem.* 1985, **134**, 165

6 Dominquez, L., Meyer, W. H. and Wegner, G. *Makromol. Chem. Rapid Commun.* 1987, **8**, 151

7 Eisenberg, A., Matsuura, H. and Yokoyama, T. *Polym. J.* 1971, **2**, 117

8 Knapick, E. G., Hirsch, J. A. and Ander, P. *Macromolecules* 1985, **18**, 1015

9 Tsutsui, T., Sato, T. and Tanaka, T. *Polym. J.* 1973, **5**, 332

10 Watanabe, M., Toneaki, N., Takizawa, Y. and Shinohara, I. *J. Polym. Sci., Polym. Chem. Edn* 1982, **20**, 2669

11 Takizawa, Y., Aiga, H., Watanabe, M. and Shinohara, I. *J. Polym. Sci., Polym. Chem. Edn* 1983, **21**, 3145

12 Takahashi, A., Kawaguchi, M., Kato, T., Kuno, M. and Matsumoto, S. *J. Macromol. Sci.-Phys. (B)* 1980, **17**, 747

13 Kohjiya, S., Ohtsuki, T. and Yamashita, S. 'Abstracts of IUPAC 6th Int. Symp. on Cationic Polymerization and Related Processes', Ghent, Belgium, 1983, p. 181

14 Hashimoto, T., Kohjiya, S. and Yamashita, S. *Nippon Gomu Kyokaishi* 1987, **60** (1), 27

15 Yamashita, S., Hashimoto, T., Yoshida, T. and Kohjiya, S. *Nippon Gomu Kyokaishi* 1987, **60** (1), 34

16 Klun, T. P., Wendling, L. A., Van Bogart, J. W. C. and Robbins, A. F. *J. Polym. Sci., Polym. Chem. Edn* 1987, **25**, 87

17 Yamashita, S., Itoi, M., Kohjiya, S. and Kidera, A. *J. Appl. Polym. Sci.* 1988, **35**, 1927

18 Sasaki, N. and Yokoyama, T. *Kobunshi Ronbunshu* 1987, **44** (12), 867

19 Leir, C. M. and Stark, J. E. *ACS Polym. Prepr.* 1988, **29** (1), 144

20 Leir, C. M. and Stark, J. E. *J. Appl. Polym. Sci.* 1989, **38** (8), 1535

21 Feng, D., Venkateshwaran, L. N., Wilkes, G. L., Leir, C. M. and Stark, J. E. *J. Appl. Polym. Sci.* 1989, **37**, 1549

22 Feng, D., Wilkes, G. L., Leir, C. M. and Stark, J. E. *J. Macromol. Sci.-Chem.* 1989, **8**, 1111

23 Feng, D. *PhD Dissertation*, Virginia Polytechnic Institute and State University, 1989

24 Kohjiya, K., Hashimoto, T., Yamashita, S. and Irie, M. *Chem. Lett.* 1985, 1497

25 Lee, B., Wilkes, G. L. and McGrath, J. E. *ACS Polym. Prepr.* 1988, **29** (1), 134

26 Lee, B. *PhD Dissertation*, Virginia Polytechnic Institute and State University, 1987

27 Feng, D., Venkateshwaran, L. N., Wilkes, G. L., Lee, B. and McGrath, J. E. *ACS Polym. Prepr.* 1988, **29** (1), 138

28 Bagrodia, S., Tant, M. R., Wilkes, G. L. and Kennedy, J. P. *Polymer* 1987, **28**, 2207

29 Tyagi, D. *PhD Dissertation*, Virginia Polytechnic Institute and State University, 1985

30 Hashimoto, T., Nagtoshi, K., Todo, A., Hasegawa, H. and Kawai, H. *Macromolecules* 1974, **7**, 364

31 Brandrup, J. and Immergut, E. H. (Eds), 'Polymer Handbook', 2nd Edn, Wiley, New York, 1974

32 Willbourn, A. H. *Trans. Faraday Soc.* 1958, **54**, 717

33 Davis, A. and Golden, J. H. *Macromol. Chem.* 1965, **81**, 38

34 Flory, P. J. 'Statistical Mechanics of Chain Molecules', Interscience, New York, 1969, pp. 170–3

35 Flory, J. P., Crescenzi, V. and Mark, J. E. *J. Am. Chem. Soc.* 1964, **86**, 146

36 Feng, D. and Wilkes, G. L. unpublished results

37 Pakula, T., Saijo, K., Kawai, H. and Hashimoto, T. *Macromolecules* 1985, **18**, 1294

38 Shibayama, M., Ohki, Y., Kotani, T. and Nomura, S. *Polym. J.* 1987, **19** (9), 1067

39 Yoo, Y., Kilic, S. and McGrath, J. E. in preparation